

Shifted-Chebyshev-polynomial-based numerical algorithm for fractional order polymer visco-elastic rotating beam

Lei Wang^a, Yi-Ming Chen^{a,b,c,*}

^a*School of Sciences, Yanshan University, Qinhuangdao, Hebei, P.R.China, 066004.*

^b*LE STUDIUM RESEARCH PROFESSOR, Loire Valley Institute for Advanced Studies, Orléans, France*

^c*INSA - Institut National des sciences appliquées - 88, Boulevard Lahitolle, Blois Cedex, France*

Abstract

In this paper, an effective numerical algorithm is proposed for the first time to solve the fractional visco-elastic rotating beam in the time domain. On the basis of fractional derivative Kelvin-Voigt and fractional derivative element constitutive models, the two governing equations of fractional visco-elastic rotating beams are established. According to the approximation technique of shifted Chebyshev polynomials, the integer and fractional differential operator matrices of polynomials are derived. By means of the collocation method and matrix technique, the operator matrices of governing equations can be transformed into the algebraic equations. In addition, the convergence analysis is performed. In particular, unlike the existing results, we can get the displacement and the stress numerical solution of the governing equation directly in the time domain. Finally, the sensitivity of the algorithm is verified by numerical examples.

Keywords: Fractional visco-elastic rotating beam, Fractional governing equation, Shifted Chebyshev polynomials, Approximation technique, Operator matrix, Numerical solution

1. Introduction

Fractional calculus and fractional differential equations have been widely used in physics, engineering, economics and other research fields [1–5], since fractional derivative has better memory [6] than integer order one, especially in the application of visco-elastic polymer materials. The fractional order constitutive model [7–12] can describe material properties more accurately with fewer parameters, so it is considered to be a good mathematical model to describe the

*Corresponding author.

Email addresses: 2414597566@qq.com (Lei Wang), chenym@ysu.edu.cn (Yi-Ming Chen)

dynamic mechanical behavior of visco-elastic materials. There are also many researches on fractional order visco-elastic beams [13–18].

The complexity of the fractional derivative determines that the numerical solution of the beam governing equation became more difficult to deal with. Scholars have used Laplace or Fourier transform to transform the time domain problem into a frequency domain problem to study the fractional order governing equation in the frequency domain. For example, Lewandowski et al. [14, 19] used fractional four-parameter model and fractional Zener model to describe visco-elastic materials. The virtual work principle and Laplace transform have been used to derive the motion equations of the considered system in the frequency domain, and then the dynamic characteristics of the visco-elastic beam have been studied. Kiasat et al. [20] used the Fourier transform to calculate the unknown coefficient of the dynamic response function to research the free vibration of isotropic visco-elastic beams and plates on visco-elastic media. The process of solving the fractional visco-elastic governing equations in the variable domain was complicated. This has led scholars to solve the analysis in the time domain.

Methods for solving fractional visco-elastic beams in the time domain include the finite element method [21, 22], multi-scale method [23], Galerkin method [24] and the variational iteration method [25] which have been found in the literature. But so far, the numerical solutions of the displacement and the stress of fractional visco-elastic rotating beams in time domain has not been studied.

As an important tool for the in-depth research and development of mathematics, function approximation theory has been successfully applied in the fields of control science and engineering, mechanical engineering, system science and so on [26–30]. It is well known that the study of numerical solutions of fractional visco-elastic beams can be attributed to the problem of solving fractional differential equations. The solutions of fractional differential equations mainly include analytical methods, polynomial approximation methods and other methods. Due to the complex form of fractional derivative, the solution of the fractional order differential equation is intractable to obtain. The analytical method has tedious numerical calculation and limited to solving some simple problems. Compared with the former, the polynomial approximation method of fractional differential equations is particularly significant because of its fast speed, high efficiency and high precision. Polynomial approximation methods include Legendre polynomial method [31, 32], Chebyshev wavelet method [33, 34], Bernoulli wavelet method [35], Bernstein polynomial method [36, 37] and shifted Chebyshev polynomials (SCPs) method [38]. The SCPs method can be used to approximate the unknown function on the extended interval, which makes it easier to solve the fractional differential equations with different physical mechanisms governing and historical background [39–42].

Rotating beams has been widely used in helicopter rotors, wind turbine blades, propellers and various rotating mechanical structures. The study of the vibration characteristics of the rotating beams [43–46] has been an important basis for the design of the rotating beam machinery. Based on this, in this paper,

we use the fractional derivative element (FDE) and the fractional derivative Kelvin-Voigt (FDKV) constitutive models. Polymers Poly(ether ether ketone) (PEEK) rotating beam and High-density polyethylene (HDPE) [47] rotating beam are studied by SCPs method. The SCPs algorithm is solved directly in the time domain, the process is simple, and the numerical solutions of the displacement and the stress of the fractional visco-elastic rotating beam can be obtained.

This paper is structured as follows, in Section 2, some preliminaries including the basic definition of fractional differential operators, the fractional visco-elastic constitutive models and the properties of SCPs are described. In Section 3, the SCPs solving algorithm is described. In Section 4, FDE model and FDKV model are used to establish two governing equations of visco-elastic rotating beam. The convergence analysis is performed in Section 5. In Section 6, the numerical results of the displacement and the stress of the visco-elastic rotating beams are obtained and discussed to show the advantages of the proposed approach. The research work in this paper is concluded in Section 7.

2. Preliminaries and notations

Some basic definitions and properties of the fractional order calculus are provided in this section.

2.1. The basic definition of fractional differential operator

Definition 1. [48] *The Caputo definition of fractional differential operator (${}^c D^\alpha f$) of order α is given by*

$$({}^c D^\alpha f)(t) = \begin{cases} \frac{1}{\Gamma(m-\alpha)} \int_0^t \frac{f^{(m)}(\tau)}{(t-\tau)^{\alpha-m+1}} d\tau, \alpha > 0, m-1 \leq \alpha < m, \\ \frac{d^m f(t)}{dt^m}, \alpha = m. \end{cases} \quad (1)$$

for the Caputo derivative, we have

$${}^c D^\alpha t^\chi = \begin{cases} 0, \text{ for } \chi \in N_0 \text{ and } \chi < \alpha, \\ \frac{\Gamma(\chi+1)}{\Gamma(\chi+1-\alpha)} t^{\chi-\alpha}, \text{ for } \chi \in N_0 \text{ and } \chi \geq \alpha \text{ or } \chi \notin N_0 \text{ and } \chi > \alpha. \end{cases} \quad (2)$$

It has following two basic properties for $m-1 \leq \alpha < m$ and $f \in L_1[a, b]$:

$$({}^c D^{\alpha c} I^\alpha f)(t) = f(t) \quad (3)$$

and

$$({}^c I^{\alpha c} D^\alpha f)(t) = f(t) - \sum_{k=0}^{m-1} f^{(k)}(0^+) \frac{(t-a)^k}{k!}, \quad t > 0 \quad (4)$$

2.2. Properties of the SCPs

SCPs are considered as useful tools to solve the fractional equation in the physical problems. The well-known Chebyshev polynomials satisfy the following term recurrence relation:

$$T_{i+1}(t) = 2tT_i(t) - T_{i-1}(t), i = 1, 2, \dots \quad (5)$$

where $T_0(t) = 1$, $T_1(t) = t$. t is defined on the interval $[-1, 1]$ and $i = 1, 2, \dots$.

On the interval $[0, L]$, where L is a non-negative real number, the SCPs are defined by the change of variable $t = \frac{2x}{L} - 1$. Let the SCPs $T_i(\frac{2x}{L} - 1)$ denote by $G_i(x)$, which can be obtained as follows:

$$G_{i+1}(x) = 2\left(\frac{2x}{L} - 1\right)G_i(x) - G_{i-1}(x), i = 1, 2, \dots \quad (6)$$

where $G_0(x) = 1$, $G_1(x) = \frac{2x}{L} - 1$. The analytic form of $G_i(x)$ of i -degree is given by:

$$G_i(x) = i \sum_{k=0}^i (-1)^{i-k} \frac{(i+k-1)!2^{2k}}{(i-k)!(2k)!L^k} x^k, i = 1, 2, \dots \quad (7)$$

where $G_i(0) = (-1)^i$ and $G_i(L) = 1$. The orthogonally condition is

$$\int_0^L G_j(x)G_k(x)\omega_L(x)dx = h_k, \quad (8)$$

where $\omega_L(x) = \frac{1}{\sqrt{Lx-x^2}}$ and $h_k = \begin{cases} \frac{b_k}{2}\pi, & k = j, \\ 0, & k \neq j, \end{cases} \quad b_0 = 2, b_k = 1, k \geq 1.$

The operational matrix is defined by:

$$\Phi_n(x) = [G_0(x), G_1(x), \dots, G_n(x)]^T \quad (9)$$

The following equation can be obtained:

$$\Phi_n(x) = A_n Z_n(x) \quad (10)$$

where $Z_n(x) = [1, x, x^2, \dots, x^n]^T$, and A_n is the SCPs coefficient matrix given as follows:

$$A_n = \begin{bmatrix} P_{0,0} & 0 & \cdots & 0 \\ P_{1,0} & P_{1,1} & \cdots & 0 \\ \vdots & \vdots & \ddots & \vdots \\ P_{n,0} & P_{n,1} & \cdots & P_{n,n} \end{bmatrix}, \quad (11)$$

where

$$\begin{cases} P_{0,0} = 1, \\ P_{i,j} = 2\left(\frac{2}{L}P_{i-1,j-1} - P_{i-1,j}\right) - P_{i-2,j}, \\ P_{i,j} = 0, \text{ for } i < j \text{ or } i < 0 \text{ or } j < 0. \end{cases}$$

Obviously, A_n is full rank and reversible.

2.3. Visco-elastic constitutive and fractional derivative models

The general form of a one-dimensional generalized fractional constitutive equation describing the stress-strain relationship of a visco-elastic material is:

$$\sum_{\kappa=0}^n \mu_{\kappa} \frac{d^{p_{\kappa}} \sigma(t)}{dt^{p_{\kappa}}} = \sum_{\kappa=0}^n \eta_{\kappa} \frac{d^{q_{\kappa}} \varepsilon(t)}{dt^{q_{\kappa}}} \quad (12)$$

where d^{κ}/dt^{κ} uses the Caputo type fractional differential definition, σ is the stress, ε is the strain, μ_{κ} , η_{κ} are the material constants. κ is a positive integer. And p_{κ} , q_{κ} are real numbers corresponding to fractional order of the time derivative.

When $p_{\kappa}, q_{\kappa} = 0$, the constitutive equation becomes ideal elastic behaviour law or Hooke's law. When $p_{\kappa} = 0, q_{\kappa} = 1$, the constitutive equation becomes ideal viscous behaviour law or Newton's law. When $0 < q_{\kappa} < 1$, the constitutive equation could be used to describe the physical behaviour of a visco-elastic material. In the current visco-elastic constitutive fractional derivative models, the first order derivatives d/dt are replaced by the fractional derivatives $d^{q_{\kappa}}/dt^{q_{\kappa}}$ with $0 < q_{\kappa} < 1$.

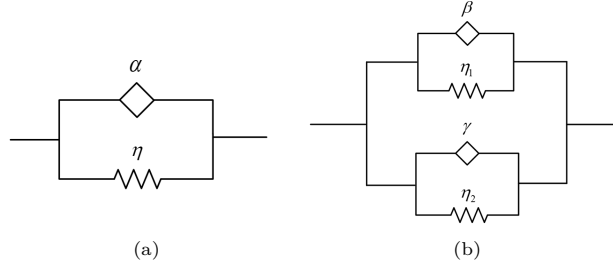


Fig. 1. Schematic representation of visco-elastic model: (a) the FDE model; (b) the FDKV model.

The simplest fractional model of visco-elastic media is the FDE model [47] as shown in Fig. 1(a), which has the following form of stress-strain relationship

$$\sigma(t) = \eta \frac{d^{\alpha} \varepsilon(t)}{dt^{\alpha}} \quad (13)$$

By replacing the elastic and viscous elements of the classical linear viscoelastic model with fractional elements, two fractional elements arranged in parallel can be obtained as shown in Fig. 1(b), which is the FDKV model [47]. And its constitutive equation as follows:

$$\sigma(t) = \eta_1 \frac{d^{\beta} \varepsilon(t)}{dt^{\beta}} + \eta_2 \frac{d^{\gamma} \varepsilon(t)}{dt^{\gamma}} \quad (14)$$

where η_1, η_2 are the material dependent constants, and $0 < \beta, \gamma < 1$.

3. Numerical algorithm

3.1. Approximation of function

For arbitrary continuous function $\omega(x, t) \in L^2([0, L] \times [0, T])$, it can be expanded as the following formula:

$$\omega(x, t) = \sum_{i=0}^{\infty} \sum_{j=0}^{\infty} \omega_{ij} G_i(x) G_j(t) \quad (15)$$

where $\omega_{ij} = \frac{1}{h_i h_j} \int_0^L \int_0^T \omega(x, t) G_i(x) G_j(t) \omega_L(x) \omega_T(t) dt dx$, $i, j = 0, 1, 2, \dots$.

If we consider truncated series in Eq. (15), then it can be rewritten as:

$$\omega(x, t) \approx \sum_{i=0}^n \sum_{j=0}^n \omega_{ij} G_i(x) G_j(t) = \Phi_n^T(x) U \Phi_n(t) \quad (16)$$

where $\Phi_n(x) = [G_0(x), G_1(x), \dots, G_n(x)]^T$, $\Phi_n(t) = [G_0(t), G_1(t), \dots, G_n(t)]^T$, $U = \{u_{ij}\}_{i,j=0}^{n,n}$.

3.2. SCPs differential operator matrix

3.2.1. First order differential operator matrix of SCPs

Definition 2. If there is matrix $P_x^{(1)}$, satisfying $\frac{d}{dx} \Phi_n(x) = P_x^{(1)} \Phi_n(x)$, then $P_x^{(1)}$ is called the first order differential operator matrix of SCPs.

By calculating the first order derivative of $\Phi_n(x)$, $\frac{d}{dx} \Phi_n(x)$ can be expressed as:

$$\begin{aligned} \frac{d}{dx} \Phi_n(x) &= (A_X Z_n(x))' = A_X Z_n'(x) \\ &= A_X \begin{bmatrix} 1' \\ x' \\ \vdots \\ (x^n)' \end{bmatrix} = A_X \begin{bmatrix} 0 \\ 1 \\ \vdots \\ nx^{n-1} \end{bmatrix} = A_X V_{(n+1) \times n} Z_n^*(x) \end{aligned} \quad (17)$$

and

$$V_{(n+1) \times n} = \begin{bmatrix} 0 & 0 & \cdots & 0 \\ 1 & 0 & \cdots & 0 \\ 0 & 2 & \cdots & 0 \\ \vdots & \vdots & \ddots & 0 \\ 0 & 0 & \cdots & n \end{bmatrix}, \quad Z_n^*(x) = \begin{bmatrix} 1 \\ x \\ \vdots \\ x^{n-2} \\ x^{n-1} \end{bmatrix} \quad (18)$$

By using Eq. (10), $Z_n^*(x)$ is obtained as:

$$Z_n^*(x) = B_X^* \Phi_n(x) \quad (19)$$

where $B_X^* = \left[A_{X, [1]}^{-1}, A_{X, [2]}^{-1}, \dots, A_{X, [n]}^{-1} \right]^T$.

According to Eq. (16), Eq. (19) can be rewritten as:

$$\frac{d}{dx} \Phi_n(x) = A_X V_{(n+1) \times n} B_X^* \Phi_n(x) \quad (20)$$

where $P_x^{(1)} = A_X V_{(n+1) \times n} B_X^*$ is a first order differential operator matrix of the SCPs. Substituting Eq. (11), Eq. (17) and matrix B_X^* into $P_x^{(1)}$:

$$P_x^{(1)} = [\lambda_0, \lambda_1, \dots, \lambda_i, \dots, \lambda_n]^T, \quad i = 0, 1, \dots, n \quad (21)$$

where $\lambda_i = \sum_{j=1}^i j P_{ij} A_{x, [j]}^{-1}$.

Now, using Eq. (16) and Eq. (20), we get:

$$\begin{aligned} \frac{\partial \omega(x, t)}{\partial x} &\approx \frac{\partial (\Phi_n^T(x) U \Phi_n(t))}{\partial x} \\ &= \Phi_n^T(x) (P_x^{(1)})^T U \Phi_n(t) \\ &= \Phi_n^T(x) (A_X V_{(n+1) \times n} B_X^*)^T U \Phi_n(t) \end{aligned} \quad (22)$$

Furthermore, the higher-order differential operator matrices derived from SCPs by mathematical induction have the following form:

$$\frac{d^n}{dx^n} \Phi_n(x) = \left(P_x^{(1)} \right)^n \Phi_n(x) \quad (23)$$

3.2.2. Fractional order differential operator matrix of the SCPs

Definition 3. If there is matrix $P_t^\beta(t)$, satisfying ${}^c D_t^\beta \Phi_n(t) = P_t^\beta(t) \Phi_n(t)$, then $P_t^\beta(t)$ is called fractional order differential operator matrix of SCPs.

By taking the fractional derivative of $\Phi_n(t)$, we obtain:

$$\begin{aligned} {}^c D_t^\beta \omega(x, t) &\approx {}^c D_t^\beta \left(\Phi_n^T(x) U \Phi_n(t) \right) \\ &= \Phi_n^T(x) U {}^c D_t^\beta \Phi_n(t) \\ &= \Phi_n^T(x) U \left[0, \dots, \frac{\Gamma(\beta+1)}{\Gamma(\beta+1-\beta)} t^{\beta-\beta}, \dots, \frac{\Gamma(i+1)}{\Gamma(i+1-\beta)} t^{i-\beta}, \dots \right]^T \\ &= \Phi_n^T(x) U A_T V_{(n+1) \times (n+1)}^\beta A_T^{-1} \Phi_n(t) \end{aligned} \quad (24)$$

where $i = \beta, \beta + 1, \dots, n$, $P_t^\beta(t) = A_T V_{(n+1) \times (n+1)}^\beta A_T^{-1}$, and

$$V_{(n+1) \times (n+1)}^\beta = \begin{bmatrix} 0 & \cdots & 0 & \cdots & 0 & \cdots & 0 \\ \vdots & \ddots & \vdots & \vdots & \vdots & \vdots & \vdots \\ 0 & \cdots & \frac{\Gamma(\beta+1)t^{-\beta}}{\Gamma(\beta+1-\beta)} & \cdots & 0 & \cdots & 0 \\ \vdots & \vdots & \vdots & \ddots & \vdots & \vdots & \vdots \\ 0 & \cdots & 0 & \cdots & \frac{\Gamma(i+1)t^{-\beta}}{\Gamma(i+1-\beta)} & \cdots & 0 \\ \vdots & \vdots & \vdots & \vdots & \vdots & \ddots & \vdots \\ 0 & \cdots & 0 & \cdots & 0 & \cdots & \frac{\Gamma(m+1)t^{-\beta}}{\Gamma(m+1-\beta)} \end{bmatrix} \quad (25)$$

The fractional order differential operator matrix $P_t^\beta(t)$ is

$$P_t^\beta(t) = \begin{bmatrix} 0 & \cdots & 0 & \cdots & 0 & \cdots & 0 \\ \vdots & \vdots & \vdots & \vdots & \vdots & \vdots & \vdots \\ 0 & \cdots & 0 & \cdots & 0 & \cdots & 0 \\ S_\beta(\beta, 0) & \cdots & S_\beta(\beta, \beta) & \cdots & 0 & \cdots & 0 \\ \vdots & \vdots & \vdots & \ddots & \vdots & \vdots & \vdots \\ S_\beta(i, 0) & \cdots & S_\beta(i, \beta) & \cdots & S_\beta(i, i) & \cdots & 0 \\ \vdots & \vdots & \vdots & \vdots & \vdots & \ddots & \vdots \\ S_\beta(n, 0) & \cdots & S_\beta(n, \beta) & \cdots & S_\beta(n, i) & \cdots & S_\beta(n, n) \end{bmatrix} \quad (26)$$

4. Establishment and solution of government equations for visco-elastic rotating beam

4.1. Beam governing equation under the FDKV model

A visco-elastic rotating beam is considered in this study. A distributed load is applied on the vertical direction of the beam. The beam is made of a visco-elastic material. The bending deformation occurs on the beam in the vertical direction, as shown in Fig. 2, in which $\omega(x, t)$ is the beam deflection, $f(x, t)$ is the distributed load, Ω is the speed and l is the length of the beam.

For visco-elastic beams, the stress and strain satisfy the two-dimensional FDKV model can be expressed as:

$$\sigma(x, t) = \eta_1 {}^c D_t^\beta \varepsilon(x, t) + \eta_2 {}^c D_t^\gamma \varepsilon(x, t) \quad (27)$$

where $\varepsilon(x, t)$ is the transverse strain, $\eta_1, \eta_2, \beta, \gamma$ are parameters of visco-elastic material, ${}^c D_t^\beta, {}^c D_t^\gamma$ use the Caputo type fractional differential definition.

The relation between the strain and the displacement can be expressed as:

$$\varepsilon(x, t) = z \frac{\partial^2 \omega(x, t)}{\partial x^2} \quad (28)$$

where x and z represent the axial and transverse coordinates.

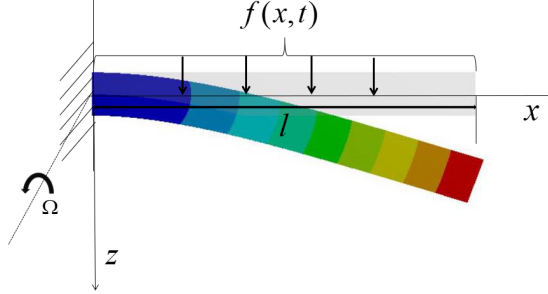


Fig. 2. The bending deformation of the visco-elastic rotating beam under distributed load.

The bending moment $M(x, t)$ of the beam is written as:

$$M(x, t) = \int_A z\sigma(x, t)dz \quad (29)$$

where $\sigma(x, t)$ is the normal stress on the cross-section.

Using Eq. (27), the beam bending moment $M(x, t)$ is equal to:

$$M(x, t) = \eta_1 I^c D_t^\beta \frac{\partial^2 \omega(x, t)}{\partial x^2} + \eta_2 I^c D_t^\gamma \frac{\partial^2 \omega(x, t)}{\partial x^2} \quad (30)$$

where I is the moment of inertia of the section given by $\int_A z^2 dA$.

The potential energy of the rotating beam is

$$U = \frac{1}{2} \int_0^L M(x, t) \frac{\partial^2 \omega(x, t)}{\partial x^2} dx + \frac{1}{2} \int_0^L T_x \frac{\partial^2 \omega(x, t)}{\partial x^2} dx \quad (31)$$

Rotating centrifugal force T_x can be expressed as:

$$T_x = \rho A \Omega^2 x \quad (32)$$

Kinetic energy is

$$T = \frac{1}{2} \int_0^L \rho A \frac{\partial^2 \omega(x, t)}{\partial t^2} dx \quad (33)$$

The beam is subjected to a load of $f(x, t)$, according to the Hamiltonian principle, we obtain that

$$\delta \int_{t_1}^{t_2} (T - U) dt + \int_{t_1}^{t_2} \delta W dt = 0 \quad (34)$$

where the work done by the external load $W = \frac{1}{2} \int_0^l f(x, t) \omega(x, t) dx$.

The governing equation of the visco-elastic rotating beam under the FDKV constitutive model is obtained:

$$\rho A \frac{\partial^2 \omega(x, t)}{\partial t^2} + \eta_1 I^C D_t^\beta \frac{\partial^4 \omega(x, t)}{\partial x^4} + \eta_2 I^C D_t^\gamma \frac{\partial^4 \omega(x, t)}{\partial x^4} - \rho A \Omega^2 x \frac{\partial^2 \omega(x, t)}{\partial x^2} = f(x, t) \quad (35)$$

4.2. Beam governing equation under the FDE model

The stress and strain satisfy the FDE constitutive model is proposed:

$$\sigma(x, t) = \eta^c D_t^\alpha \varepsilon(x, t) \quad (36)$$

According to Eq. (36), the beam bending moment $M(x, t)$ can be rewritten as:

$$M(x, t) = \eta I^c D_t^\alpha \frac{\partial^2 \omega(x, t)}{\partial x^2} \quad (37)$$

where I is the moment of inertia of the section given by $\int_A z^2 dA$.

The governing equation of the visco-elastic rotating beam under the FDKV constitutive model is obtained as follows:

$$\rho A \frac{\partial^2 \omega(x, t)}{\partial t^2} + \eta I^c D_t^\alpha \frac{\partial^4 \omega(x, t)}{\partial x^4} - \rho A \Omega^2 x \frac{\partial^2 \omega(x, t)}{\partial x^2} = f(x, t) \quad (38)$$

4.3. The solution of governing equation based on SCPs

Based on integer order differential operator matrix of SCPs in the Section 3.2.1, the following equations can be obtained:

$$\begin{aligned} \frac{\partial^2 \omega(x, t)}{\partial x^2} &\approx \frac{\partial^2 (\Phi_n^T(x) U \Phi_n(t))}{\partial x^2} \\ &= \Phi_n^T(x) ((P_x^{(1)})^T)^2 U \Phi_n(t) \\ &= \Phi_n^T(x) ((A_X V_{(n+1) \times n} B_X^*)^T)^2 U \Phi_n(t) \end{aligned} \quad (39)$$

$$\begin{aligned} \frac{\partial^4 \omega(x, t)}{\partial x^4} &\approx \frac{\partial^4 (\Phi_n^T(x) U \Phi_n(t))}{\partial x^4} \\ &= \Phi_n^T(x) ((P_x^{(1)})^T)^4 U \Phi_n(t) \\ &= \Phi_n^T(x) ((A_X V_{(n+1) \times n} B_X^*)^T)^4 U \Phi_n(t) \end{aligned} \quad (40)$$

$$\begin{aligned} \frac{\partial^2 \omega(x, t)}{\partial t^2} &\approx \frac{\partial^2 (\Phi_n^T(x) U \Phi_n(t))}{\partial t^2} \\ &= \Phi_n^T(x) U (P_t^{(1)})^2 \Phi_n(t) \\ &= \Phi_n^T(x) U (A_T V_{(n+1) \times n} B_T^*)^2 \Phi_n(t) \end{aligned} \quad (41)$$

By the fractional order differential operator matrix of SCPs in the Section

3.2.2, the following equations can be obtained:

$$\begin{aligned}
{}^c D_t^\beta \frac{\partial^4 \omega(x, t)}{\partial x^4} &\approx {}^c D_t^\beta \Phi_n^T(x) \left((A_X V_{(n+1) \times n} B_X^*)^T \right)^4 U \Phi_n(t) \\
&= \Phi_n^T(x) \left((A_X V_{(n+1) \times n} B_X^*)^T \right)^4 U {}^c D_t^\beta \Phi_n(t) \\
&= \Phi_n^T(x) \left((A_X V_{(n+1) \times n} B_X^*)^T \right)^4 U A_T P_t^\beta(t) A_T^{-1} \Phi_n(t)
\end{aligned} \tag{42}$$

Similarly,

$$\begin{aligned}
{}^c D_t^\gamma \frac{\partial^4 \omega(x, t)}{\partial x^4} &\approx {}^c D_t^\gamma \Phi_n^T(x) \left((A_X V_{(n+1) \times n} B_X^*)^T \right)^4 U \Phi_n(t) \\
&= \Phi_n^T(x) \left((A_X V_{(n+1) \times n} B_X^*)^T \right)^4 U {}^c D_t^\gamma \Phi_n(t) \\
&= \Phi_n^T(x) \left((A_X V_{(n+1) \times n} B_X^*)^T \right)^4 U A_T P_t^\gamma(t) A_T^{-1} \Phi_n(t)
\end{aligned} \tag{43}$$

where $P_t^\gamma(t)$ is obtained by replacing β with γ in Eq. (26).

The governing equation Eq. (35) can be rewritten into the operator matrix form as follows:

$$\begin{aligned}
&\rho A \Phi_n^T(x) U \left(P_t^{(1)} \right)^2 \Phi_n(t) + \eta_1 I \Phi_n^T(x) \left((P_x^{(1)})^T \right)^4 U P_t^\beta(t) \Phi_n(t) \\
+ \eta_2 I \Phi_n^T(x) \left((P_x^{(1)})^T \right)^4 U P_t^\gamma(t) \Phi_n(t) - \rho A \Omega^2 x \Phi_n^T(x) \left((P_x^{(1)})^T \right)^2 U \Phi_n(t) &= f(x, t)
\end{aligned} \tag{44}$$

Specifically, Eq. (44) can be written as:

$$\begin{aligned}
\rho A \Phi_n^T(x) U (A_T V_{(n+1) \times n} B_T^*)^2 \Phi_n(t) + \eta_1 I \Phi_n^T(x) \left((A_X V_{(n+1) \times n} B_X^*)^T \right)^4 U A_T \times \\
V_{(n+1) \times (n+1)}^\beta A_T^{-1} \Phi_n(t) + \eta_2 I \Phi_n^T(x) \left((A_X V_{(n+1) \times n} B_X^*)^T \right)^4 U A_T \times \\
V_{(n+1) \times (n+1)}^\gamma A_T^{-1} \Phi_n(t) - \rho A \Omega^2 x \left((A_X V_{(n+1) \times n} B_X^*)^T \right)^2 U \Phi_n(t) &= f(x, t)
\end{aligned} \tag{45}$$

Similarly, the governing equation Eq. (38) can be rewritten into the operator matrix form as follows:

$$\begin{aligned}
\rho A \Phi_n^T(x) U \left(P_t^{(1)} \right)^2 \Phi_n(t) + \eta I \Phi_n^T(x) \left((P_t^{(1)})^T \right)^4 U P_t^\alpha(t) \Phi_n(t) \\
- \rho A \Omega^2 x \Phi_n^T(x) \left((P_x^{(1)})^T \right)^2 U \Phi_n(t) &= f(x, t)
\end{aligned} \tag{46}$$

The Eq. (46) can be written as:

$$\begin{aligned}
\rho A \Phi_n^T(x) U (A_T V_{(n+1) \times n} B_T^*)^2 \Phi_n(t) + \eta I \Phi_n^T(x) \left((A_X V_{(n+1) \times n} B_X^*)^T \right)^4 U A_T \times \\
V_{(n+1) \times (n+1)}^\alpha A_T^{-1} \Phi_n(t) - \rho A \Omega^2 x \left((A_X V_{(n+1) \times n} B_X^*)^T \right)^2 U \Phi_n(t) &= f(x, t)
\end{aligned} \tag{47}$$

where $P_t^\alpha(t)$ is obtained by replacing β with α in Eq. (26).

Based on the collocation method, the reasonable match points $x_i = \frac{2i-1}{2(n+1)}L$, $i = 0, 1, 2, \dots, n$, $t_j = \frac{2j-1}{2(n+1)}T$, $j = 0, 1, 2, \dots, n$ have been used to discretize the variable (x, t) to (x_i, t_j) . Eq. (35) and Eq. (38) are transformed into a set of algebraic equations. The coefficient $\omega_{i,j}$ ($i = 1, 2, \dots, n; j = 1, 2, \dots, n$) is determinate by using Matlab platform and least square method. The numerical solution of the fractional derivative equations can be obtained.

5. Convergence analysis

In this section, for any function, the norm is defined as

$$\|\omega(x, t)\| = \sup_{(x,t) \in \Lambda} |\omega(x, t)| \quad (48)$$

Theorem 1. Suppose $\omega(x, t) \in C^3(\Lambda)$, $\omega(x, t)$ is the exact solution of the fractional governing equation, $\omega_n(x, t)$ is the numerical solution. Then the error bound is

$$\|e_n(x, t)\| = \|\omega(x, t) - \omega_n(x, t)\| \leq Nh^3 = O(h^3) \quad (49)$$

Proof 1. Let

$$e_{n,ij}(x, t) = \begin{cases} \omega(x, t) - \omega_n(x, t) & (x, t) \in \Lambda_n \\ 0 & (x, t) \in \Lambda - \Lambda_n \end{cases} \quad (50)$$

where $\Lambda_n = \{(x, t) | ih \leq x < (i+2)h, jh \leq t < (j+2)h, i, j = 0, 2, \dots, n-2\}$. $\omega_n(x, t)$ is the quadratic polynomial interpolation function on $\omega(x, t)$ on Λ_n . Then,

$$\begin{aligned} e_{n,ij}(x, t) &= \frac{1}{6} \frac{\partial^3 \omega(\xi_{1,i}, t)}{\partial x^3} \prod_{i'=i}^{i+2} (x - x_{i'}) + \frac{1}{6} \frac{\partial^3 \omega(x, \zeta_{1,j})}{\partial t^3} \prod_{j'=j}^{j+2} (t - t_{j'}) \\ &\quad - \frac{1}{36} \frac{\partial^6 \omega(\xi_{2,i}, \zeta_{2,j})}{\partial x^3 \partial t^3} \prod_{i'=i}^{i+2} (x - x_{i'}) \prod_{j'=j}^{j+2} (t - t_{j'}) \end{aligned} \quad (51)$$

where $x, \xi_{1,i}, \xi_{2,i} \in [x_i, x_{i+2})$, and $t, \zeta_{1,j}, \zeta_{2,j} \in [t_j, t_{j+2})$, $i, j = 0, 2, \dots, n-2$.

So,

$$\begin{aligned}
\|e_{n,ij}(x, t)\| &= \frac{1}{6} \left\| \frac{\partial^3 \omega(\xi_{1,i}, t)}{\partial x^3} \right\| \left\| \prod_{i'=i}^{i+2} (x - x_{i'}) \right\| \\
&\quad + \frac{1}{6} \left\| \frac{\partial^3 \omega(x, \zeta_{1,j})}{\partial t^3} \right\| \left\| \prod_{j'=j}^{j+2} (t - t_{j'}) \right\| \\
&\quad + \frac{1}{36} \left\| \frac{\partial^6 \omega(\xi_{2,i}, \zeta_{2,j})}{\partial x^3 \partial t^3} \right\| \left\| \prod_{i'=i}^{i+2} (x - x_{i'}) \right\| \left\| \prod_{j'=j}^{j+2} (t - t_{j'}) \right\|
\end{aligned} \tag{52}$$

where $\left\| \prod_{i'=i}^{i+2} (x - x_{i'}) \right\| = \sup_{x \in [x_i, x_{i+2}]} \left| \prod_{i'=i}^{i+2} (x - x_{i'}) \right|$.

According to $\left| \prod_{i'=i}^{i+2} (x - x_{i'}) \right|$ is the maximum value of $x = (i + 1 - \frac{\sqrt{3}}{3})h$, we can get:

$$\left\| \prod_{i'=i}^{i+2} (x - x_{i'}) \right\| \leq \frac{2\sqrt{3}h^3}{9}, \forall x \in [x_i, x_{i+2}] \tag{53}$$

$$\left\| \prod_{j'=j}^{j+2} (t - t_{j'}) \right\| \leq \frac{2\sqrt{3}h^3}{9}, \forall t \in [t_j, t_{j+2}] \tag{54}$$

Substituting Eq. (53) and Eq. (54) into Eq. (52), we can get:

$$\begin{aligned}
\|e_n(x, t)\| &\leq \frac{\sqrt{3}h^3}{27} \left(\left\| \frac{\partial^3 \omega(x, t)}{\partial x^3} \right\| + \left\| \frac{\partial^3 \omega(x, t)}{\partial t^3} \right\| + \frac{\sqrt{3}h^3}{27} \left\| \frac{\partial^6 \omega(x, t)}{\partial x^3 \partial t^3} \right\| \right) \\
&= Nh^3 = O(h^3)
\end{aligned} \tag{55}$$

In summary, the theorem is proved.

6. Numerical analysis

Based on HDPE, PEEK and rock creep experimental data, Xu et al. [47] used the interior point method to solve the corresponding nonlinear optimization constraint problem. The best simulation parameters of FDE model, fractional Maxwell model, FDKV model and fractional Poynting-Thomson model were

obtained. This paper uses HDPE and PEEK to have the best simulation parameters [47] of the FDE model and the parameters of HDPE in the FDKV model as Tab. 1 and Tab. 2.

Table 1 The best simulation parameters of HDPE and PEEK under FDE constitutive model.

Material	β	γ	η_1	η_2
HDPE	0.3320	0.1088	$2.874 \times 10^5 Pa$	$1.558 \times 10^5 Pa$

Table 2 The best simulation parameters of HDPE under FDKV constitutive model.

Material	α	η
HDPE	0.1603	$3.341 \times 10^5 Pa$
PEEK	0.2341	$5.50 \times 10^6 Pa$

Let the beam length $l = 2.5m$ and the cross-section area $A = 0.04m^2$. Moment of inertia $I = \frac{(0.2)^4}{12}$. Based on SCPs method, the numerical solutions of the displacement of the visco-elastic rotating beams under the FDE model and the FDKV model are solved. Assuming that the visco-elastic beam is a cantilever beam, the boundary conditions and initial conditions are

$$\begin{cases} \omega(0, t) = \frac{\partial \omega(0, t)}{\partial x} = 0 \\ \frac{\partial^2 \omega(l, t)}{\partial x^2} = \frac{\partial^3 \omega(l, t)}{\partial x^3} = 0 \\ \omega(x, 0) = 0, \frac{\partial \omega(x, 0)}{\partial t} = 0 \end{cases} \quad (56)$$

6.1. Numerical solutions of HDPE beam under FDKV model

In this section, the displacements of HDPE rotating beam under different loads under FDKV model are discussed. When $\Omega = 0$, there is no rotational force. Fig. 3 shows the displacements of the non-rotating beam under different uniform loads, simple harmonic loads and linear loads when $t = 0.5s$. Fig. 4 shows the displacements of HDPE rotating beam under different uniform loads, simple harmonic loads and linear loads when rotating speed $\Omega = \pi/2$.

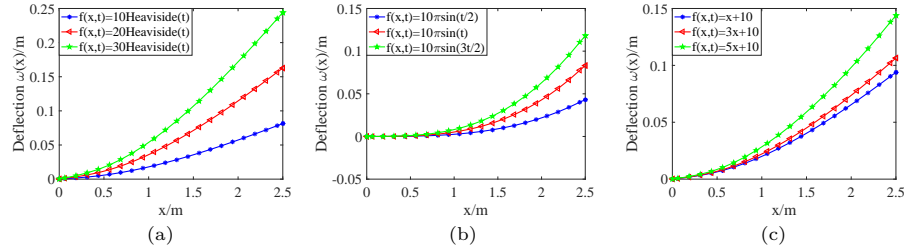


Fig. 3. Displacements of HDPE non-rotating beams under different external loads: (a) Uniform loads; (b) Simple harmonic loads; (c) Linear loads.

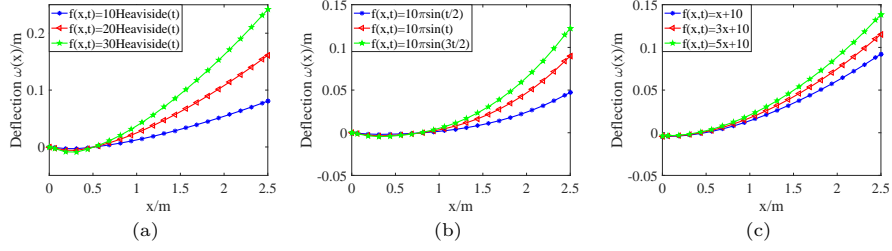


Fig. 4. Displacements of HDPE rotating beam at $\Omega = \frac{\pi}{2}$ under different external loads: (a) Uniform loads; (b) Simple harmonic loads; (c) Linear loads.

From Fig. 3, we can get that the displacements of the HDPE non-rotating beam gradually increases with time under the loads. At the same position, as the load increases, the displacement gradually increases. And the same conclusions can also be obtained by means of Fig. 4. In [49], a Fourier series is constructed and supplemented by a boundary smoothing term to express the displacement of the rotating beam. The governing equation of Ref.[49] can be considered as the governing Eq. (38) when α is fraction. Fig. 3 and Fig. 4 are similar to the results of Ref.[49]. Compared with Ref.[49], the numerical result is verified to be correct. In addition, we can clearly see that the displacements of HDPE beam changes with the rotation speed.

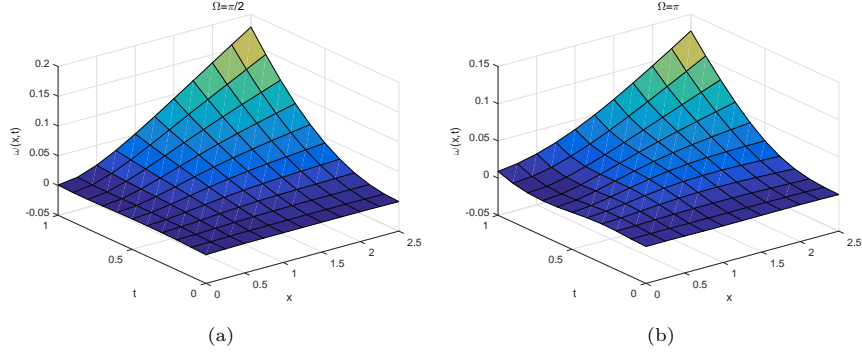


Fig. 5. Displacements of HDPE rotating beam under external load $f(x,t) = 10Heaviside(t)$ at different rotational speeds: (a) $\Omega = \frac{\pi}{2}$; (b) $\Omega = \pi$.

Fig. 5 shows the numerical solutions of the displacement of the HDPE rotating beam at rotating speeds of $\Omega = \frac{\pi}{2}$, $\Omega = \pi$ under the external load $f(x,t) = 10Heaviside(t)$. It can be seen from the image that the proposed algorithm has a good simulation effect to solve such problems, and the feasibility of the algorithm is verified.

However, in the case of slight deformation, the transverse strain of the neu-

tral surface can be expressed as:

$$\varepsilon = \frac{\partial^2 \omega(x, t)}{\partial x^2} \quad (57)$$

According to Eq. (27), the stress can be obtained:

$$\sigma(x, t) = \eta_1 {}^c D_t^\beta \frac{\partial^2 \omega(x, t)}{\partial x^2} + \eta_2 {}^c D_t^\gamma \frac{\partial^2 \omega(x, t)}{\partial x^2} \quad (58)$$

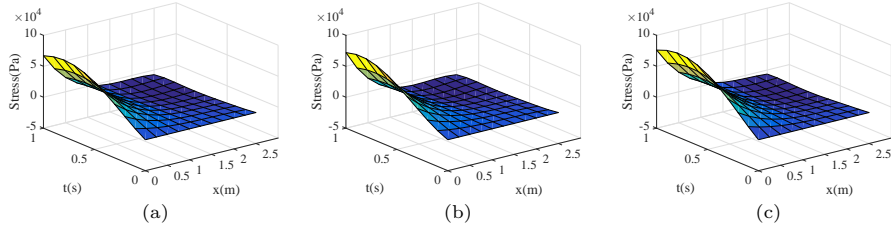


Fig. 6. The stress of HDPE rotating beam at $\Omega = \frac{\pi}{2}$ under different external loads: (a) Uniform load $f(x, t) = 10\text{Heaviside}(t)$; (b) Simple harmonic load $f(x, t) = 10\pi\sin(t)$; (c) Linear load $f(x, t) = 10 + 2x$.

Fig. 6 shows the stress of the HDPE rotating beam at the different external loads when the rotational speed $\Omega = \frac{\pi}{2}$. Through the images, we can clearly see that the closer to the fixed end of the beam, the greater the stress. Therefore, the stronger the resistance to external force deformation near $x = 0$, the smaller the displacement. This is consistent with the change in the displacement map above. The accuracy and feasibility of the algorithm are further verified.

6.2. Comparison HDPE beams and PEEK beams

The displacement solutions of HDPE beam and PEEK beam under different loads of the FDE constitutive model are discussed and compared in this section.

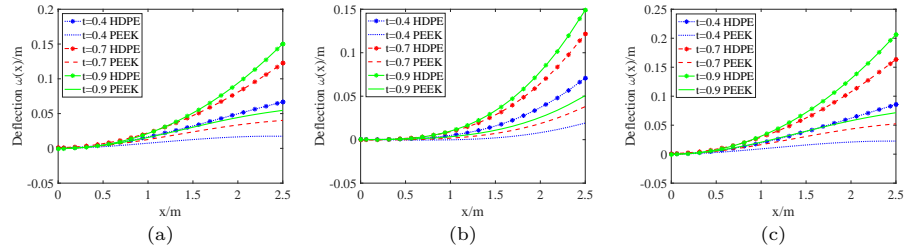


Fig. 7. Comparison of displacements between HDPE non-rotating beam and PEEK non-rotating beam under different external loads: (a) Uniform load $f(x, t) = 10\text{Heaviside}(t)$; (b) Simple harmonic load $f(x, t) = 10\pi\sin(t)$; (c) Linear load $f(x, t) = 10 + 2x$.

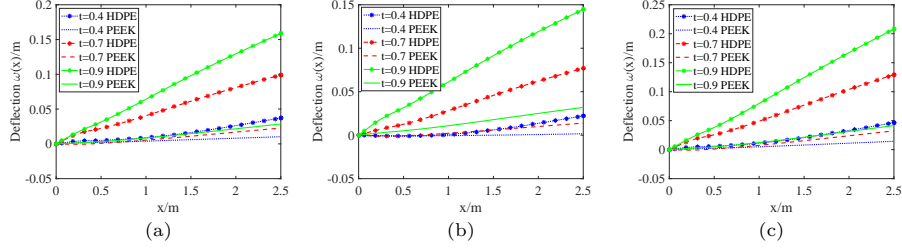


Fig. 8. Comparison of displacements between HDPE rotating beam and PEEK rotating beam at $\Omega = \frac{\pi}{2}$ under different external loads: (a) Uniform load $f(x, t) = 10\text{Heaviside}(t)$; (b) Simple harmonic load $f(x, t) = 10\pi\sin(t)$; (c) Linear load $f(x, t) = 10 + 2x$.

Obviously, as can be seen from Fig. 7 and Fig. 8, the displacement of the PEEK beam is less than the displacement of the HDPE beam when the rotational speed and the external load are constant. The smaller the displacement, the greater the damping of the corresponding visco-elastic material and the better the bending resistance. Therefore, the PEEK beam have better bending resistance than the HDPE beam. The results obtained are consistent with the actual material properties. The proposed algorithm calculates the displacement solution well and has high precision. Thus, this method can provide a theoretical basis for the research, development and performance prediction of damping materials.

7. Conclusion

In this paper, an effective numerical algorithm for solving fractional visco-elastic rotating beam based on SCPs is proposed for the first time in the time domain. The displacements of visco-elastic beam can reflect the positional changes of beam at different times. The fractional derivative model is used to analyze the inherent laws of the dynamic performance of visco-elastic damping materials, which can provide a theoretical basis for the research, development and performance prediction of damping materials.

1. Two governing equations of fractional visco-elastic rotating beam are established by FDE and FDKV constitutive models, the dynamic equation of beam and strain-displacement relationship.
2. According to the properties of SCPs, the integer and fractional differential operator matrices of polynomials are derived. Using the polynomial to approximate the unknown function, the fractional order governing equation is rewritten into the form of matrix product. The variables are discretized based on the collocation method, and the original problem is transformed into an algebraic equation system. The numerical solutions of the governing equations can be obtained directly in the time domain.
3. Numerical examples show the displacement and stress changes of HDPE rotating beam under uniform load, harmonic load and linear load under FDKV constitutive model, and further verify the effectiveness and

feasibility of the algorithm. By comparing the displacement of different viscoelastic beams, HDPE rotating beam and PEEK rotating beam, the properties of materials are analyzed theoretically.

Acknowledgments

This work is supported by the Natural Science Foundation of Hebei Province (A2017203100) in China and the LE STUDIUM RESEARCH PROFESSOR-SHIP award of Centre-Val de Loire region in France.

References

- [1] Sweilam NH, Almekhlafi SM. Numerical study for multi-strain tuberculosis (TB) model of variable-order fractional derivatives[J]. *Journal of Advanced Research*. 2016, 7(2): 271–283.
- [2] Ramirez, Coimbra. A variable order constitutive relation for viscoelasticity[J]. *Annalen Der Physik*. 2010, 16(7-8): 543–552.
- [3] Lorenzo CF, Hartley TT. Initialization, conceptualization, and application in the generalized (fractional) calculus[J]. *Critical Reviews in Biomedical Engineering*. 2007, 35(6): 447–553.
- [4] Meerschaert MM, Scalas E. Coupled continuous time random walks in finance[J]. *Physica A Statistical Mechanics And Its Applications*. 2006, 370(1): 114–118.
- [5] Chen W. Nonlinear dynamics and chaos in a fractional-order financial system[J]. *Chaos Solitons and Fractals*. 2008, 36(5): 1305–1314.
- [6] Du M, Wang Z, Hu H. Measuring memory with the order of fractional derivative[J]. *Scientific Reports*. 2013, 3(7478):3431.
- [7] Gemant A. On fractional differences[J]. *Phil Mag*. 1938, 25(1):92–96.
- [8] Bagley RL, Torvik PJ. On the fractional calculus model of viscoelasticity behavior[J]. *Journal of Rheology*. 1986, 30(1):133–155.
- [9] Leung AYT, Yang HX, Zhu P, Guo ZJ. Steady state response of fractionally damped nonlinear viscoelastic arches by residue harmonic homotopy[J]. *Computers and Structures*. 2013, 121(5):10–21.
- [10] Lewandowski R, Pawlak Z. Dynamic analysis of frames with viscoelastic dampers modelled by rheological models with fractional derivatives[J]. *Journal of Sound and Vibration*. 2011, 330(5):923–936.
- [11] Kang JH, Zhou FB, Liu C, Liu YK. A fractional nonlinear creep model for coal considering damage effect and experimental validation[J]. *International Journal of Non-Linear Mechanics*. 2015, 76:20–28.

- [12] Gioacchino A, Mario DP, Giuseppe F. On the dynamics of non-local fractional viscoelastic beams under stochastic agencies[J]. *Composites Part B: Engineering*. 2018, 131:102–110.
- [13] Lewandowski R, Wielentejczyk P. Nonlinear vibration of viscoelastic beams described using fractional order derivatives[J]. *Journal of Sound and Vibration*. 2017, 339(2):228–243.
- [14] Lewandowski R, Baum M. Dynamic characteristics of multilayered beams with viscoelastic layers described by the fractional Zener model[J]. *Archive of Applied Mechanics*. 2015, 85(12):1793–1814.
- [15] Cortes F, Elejabarrieta MJ. Finite element formulations for transient dynamic analysis in structural systems with viscoelastic treatments containing fractional derivative models[J]. *International Journal for Numerical Methods in Engineering*. 2007, 69(10):2173–2195.
- [16] Bahraini SMS, Farid M, Ghavanloo E. Large deflection of viscoelastic beams using fractional derivative model[J]. *Journal of Engineering Mathematics*. 2013, 27(4):1063–1070.
- [17] Paola MD, Heuer R, Pirrotta A. Fractional visco-elastic Euler–Bernoulli beam[J]. *International Journal of Solids and Structures*. 2013, 50(22-23):3505–3510.
- [18] He XQ, Rafiee M, Mareishi S, Liew KM. Large amplitude vibration of fractionally damped viscoelastic CNTs/fiber/polymer multiscale composite beams[J]. *Composite Structures*. 2015, 131:1111–1123.
- [19] Magdalena LP, Lewandowski R. Sensitivity Analysis of Dynamic Characteristics of Composite Beams with Viscoelastic Layers[J]. *Procedia Engineering*. 2017, 199:366–371.
- [20] Kiasat MS, Zamani HA, Aghdam MM. On the transient response of viscoelastic beams and plates on viscoelastic medium[J]. *International Journal of Mechanical Sciences*. 2014, 83(7-8):133–145.
- [21] Chang JR, Lin WJ, Huang CJ, Choi ST. Vibration and stability of an axially moving Rayleigh beam[J]. *Applied Mathematical Modelling*. 2010, 34(6):1482–1497.
- [22] Friswell MI, Adhikari S, Lei Y. Vibration analysis of beams with non-local foundations using the finite element method[J]. *International Journal for Numerical Methods in Engineering*. 2007, 71(11):1365–1386.
- [23] Demir DD, Bildik N, Sınır BG. Linear dynamical analysis of fractionally damped beams and rods[J]. *Journal of Engineering Mathematics*. 2014, 85(1):131–147.

- [24] Permoon MR, Rashidinia J, Parsa A, Haddadpour H, Salehi R. Application of radial basis functions and sinc method for solving the forced vibration of fractional viscoelastic beam[J]. *Journal of Mechanical Science and Technology*. 2016, 30(7):3001–3008.
- [25] Martin O. A modified variational iteration method for the analysis of viscoelastic beams[J]. *Applied Mathematical Modelling*. 2016, 40(17):7988–7995.
- [26] Akritas P, Antoniou I, Ivanov VV. Identification and prediction of discrete chaotic maps applying a Chebyshev neural network[J]. *Chaos, Solitons and Fractals*. 2000, 11(1-3):337–344.
- [27] Sun KK, Mou SS, Qiu JB, Wang T, Gao HJ. Adaptive Fuzzy Control for Non-Triangular Structural Stochastic Switched Nonlinear Systems with Full State Constraints[J]. *IEEE Transactions on Fuzzy Systems*. 2019, 27(8):1587–1601.
- [28] Qiu JB, Sun KK, Wang T, Gao HJ. Observer-Based Fuzzy Adaptive Event-Triggered Control for Pure-Feedback Nonlinear Systems with Prescribed Performance[J]. *IEEE Transactions on Fuzzy Systems*. 2019, 27(11):2152–2161.
- [29] Qiu JB, Sun KK, Rudas IJ, Gao HJ. Command Filter-Based Adaptive NN Control for MIMO Nonlinear Systems With Full-State Constraints and Actuator Hysteresis[J]. *IEEE Transactions on Fuzzy Systems*. 2019, 1–11.
- [30] Tadjeran C, Mark M. Meerschaert and Hans-Peter Scheffler. A second-order accurate numerical approximation for the fractional diffusion equation[J]. *Journal of Computational Physics*. 2006, 213(1):205–213.
- [31] Meng ZJ, Yi MX, Huang J, Lei S. Numerical solutions of nonlinear fractional differential equations by alternative Legendre polynomials[J]. *Applied Mathematics and Computation*. 2018, 336:454–464.
- [32] Chen YM, Sun YN, Liu LQ. Numerical solution of fractional partial differential equations with variable coefficients using generalized fractional-order Legendre functions[J]. *Applied Mathematics and Computation*. 2014, 244(2):847–858.
- [33] Xie JQ, Yao ZB, Gui HL, Zhao FQ, Li DY. A two-dimensional Chebyshev wavelets approach for solving the Fokker-Planck equations of time and space fractional derivatives type with variable coefficients[J]. *Applied Mathematics and Computation*. 2018, 332:197–208.
- [34] Chen YM, Sun L, Li X, Fu XH. Numerical solution of nonlinear fractional integral differential equations by using the second kind Chebyshev wavelets[J]. *Computer Modeling in Engineering and Sciences*. 2013, 90(5):359–378.
- [35] Wang J, Xu TZ, Wei YQ, Xie JQ. Numerical solutions for systems of fractional order differential equations with Bernoulli wavelets[J]. *International Journal of Computer Mathematics*. 2018, 96(2):317–336.

- [36] Chen YM, Liu LQ, Liu DY, Boutat D. Numerical study of a class of variable order nonlinear fractional differential equation in terms of Bernstein polynomials[J]. *Ain Shams Engineering Journal*. 2016,1235–1241.
- [37] Chen YM, Liu LQ, Li BF, Sun YN. Numerical solution for the variable order linear cable equation with Bernstein polynomials[J]. *Applied Mathematics and Computation*. 2014, 238(7):329–341.
- [38] Fernanda SP, Miguel P, Higinio R. Extrapolating for attaining high precision solutions for fractional partial differential equations[J]. *Fractional Calculus and Applied Analysis*. 2018, 21(6):1506–1523.
- [39] Suman S, Kumar A, Singh GK. A new method for higher-order linear phase FIR digital filter using shifted Chebyshev polynomials[J]. *Signal Image and Video Processing*. 2016, 10(6):1041–1048.
- [40] Zaicenco AG. Sensitivity analysis of a seismic risk scenario using sparse Chebyshev polynomial expansion[J]. *Geophysical Journal International*. 2015, 200(3):1466–1482.
- [41] Xing S, Guo HW. Temporal phase unwrapping for fringe projection profilometry aided by recursion of Chebyshev polynomials[J]. *Applied Optics*. 2017, 56(6):1591–1602.
- [42] Protasov V, Jungers R. Analysing the Stability of Linear Systems via Exponential Chebyshev Polynomials[J]. *IEEE Transactions on Automatic Control*. 2016, 61(3):795–798.
- [43] Srivatsa BK, Ganguli R. Non-rotating beams isospectral to rotating Rayleigh beams[J]. *International Journal of Mechanical Sciences*. 2018, 142-143:440–455.
- [44] Tian JJ, Su JP, Kai Z, Hua HX. A modified variational method for nonlinear vibration analysis of rotating beams including Coriolis effects[J]. *Journal of Sound and Vibration*. 2018, 426:258–277.
- [45] Bazoune A. Effect of tapering on natural frequencies of rotating beams[J]. *Shock and Vibration*. 2014, 14(14):169–179.
- [46] Banerjee JR, Su H, Jackson DR. Free vibration of rotating tapered beams using the dynamic stiffness method[J]. *Journal of Sound and Vibration*. 2006, 298(4):1034–1054.
- [47] Xu HY, Jiang XY. Creep constitutive models for viscoelastic materials based on fractional derivatives[J]. *Computers and Mathematics with Applications*. 2017, 73(6):1377–1384.
- [48] Lin YM, Xu CJ. Finite difference/spectral approximations for the time-fractional diffusion equation[J]. *Journal of Computational Physics*. 2007, 255(2):1533–1552.

- [49] Chen Q, Du JT. A Fourier series solution for the transverse vibration of rotating beams with elastic boundary supports[J]. *Applied Acoustics*. 2019, 155:1–15.